JCTC Journal of Chemical Theory and Computation

Evaluation of Electronic Coupling in Transition-Metal Systems Using DFT: Application to the Hexa-Aquo Ferric−Ferrous Redox Couple

Agostino Migliore,* Patrick H.-L. Sit,* and Michael L. Klein

Center for Molecular Modeling and Department of Chemistry, University of Pennsylvania, 231 South 34th Street, Philadelphia, Pennsylvania 19104-6323

Received August 16, 2008

Abstract: We present a density-functional theory (DFT) approach, with fractionally occupied orbitals, for studying the prototypical ferric−ferrous electron-transfer (ET) process in liquid water. We use a recently developed ab initio method to calculate the transfer integral (also named electronic-coupling or ET matrix element) between the solvated ions. The computed transfer integral is combined with previous ab initio values of the reorganization energy, within the framework of Marcus' theory, to estimate the rate of the electron self-exchange reaction. The self-interaction correction incorporated (through an appropriate treatment of the electronic correlation effects) into a Hubbard *U* extension to the DFT scheme leads to a theoretical value of the ET rate relatively close to an experimental estimate from kinetic measurements. The use of fractional occupation numbers (FON) turned out to be crucial for achieving convergence in most self-consistent calculations because of the open-shell d-multiplet electronic structure of each iron ion and the near degeneracy of the redox groups involved. We provide a theoretical justification for the FON approach, which allows a description of the chemical potential and orbital relaxation, and possible extension to other transition-metal redox systems. Accordingly, the methodology developed in this paper, which rests on a suitable combination of Hubbard *U* correction and a FON approach to DFT, seems to offer a fruitful approach for the quantitative description of ET reactions in biochemical systems.

1. Introduction

ET reactions play an essential role in inorganic and organic redox chemistry. In particular, a wide variety of reactions relevant to chemistry and molecular electronics involve nonadiabatic ET processes.[1] The $Fe^{2+}-Fe^{3+}$ redox couple is an archetypal system for the theoretical analysis of homogeneous ET reactions[2−6] and is relevant in many practical contexts, such as corrosion studies and environmental remediation strategies.[7−9]

ET reactions are characterized by means of their rate constants (conductance in molecular electronics applications[10]) and the relevant electron-tunneling pathways. Within the general context of Marcus' ET theory,[11] the rate constant of nonadiabatic ET reactions is essentially controlled by three key quantities: the reorganization energy (i.e., the free energy change due to the nuclear rearrangement that follows the ET process), the nuclear frequency factor (the frequency of the crossover through the transition-state barrier), and the electronic transmission coefficient or electronic factor. The latter can be strongly dependent on the transfer integral,[12] which is the effective electronic coupling between the donor and acceptor redox groups. In particular, according to the Landau−Zener model[13,14] the electronic factor is proportional to the square modulus of the transfer integral for ET reactions in the nonadiabatic limit.

The resultant expression of the nonadiabatic electron-transfer rate at a given temperature depends on the reorganization energy and the transfer integral. The latter provides a compact link between the ET rates and the electronic

* Corresponding author phone: 215-898-7058; fax: 215-573-6233; e-mail: amigliore@cmm.upenn.edu.

10.1021/ct800340v CCC: $40.75
Published on Web 01/15/2009

properties of the interacting redox groups. Since electronic structure plays a pivotal role in determining the kinetics of ET reactions,[15] considerable effort has been devoted to computing electronic couplings by means of several quantum chemical methods.[16−23] Nevertheless, transfer integrals are often very small and thus difficult to compute with high accuracy. As to the system under study, an accurate estimation of the electronic coupling is further complicated by the multiplet nature of the system. Moreover, it is expected[5] that the transfer integral, and the ET rate, is sensitive to the configuration of the solvation water molecules around the two metal ions. In fact, water molecules can have a dramatic effect on the ET kinetics, resulting from the interplay[24,25] between the water−ion electrostatic interactions (which can either promote or oppose the electron transfer as a consequence of the water arrangement) and the effectiveness of the water molecules between the two redox centers in mediating ET coupling pathways. (For any redox system, the latter amounts to a favorable contribution, lowering the barrier for electron tunneling relative to the vacuum.[26])

Two noteworthy estimates of the transfer integral for the $Fe^{2+}-Fe^{3+}$ redox couple (refs 3 and 5) provide benchmark evaluations of the transfer integral. A more recent approach[27] uses a quasi-experimental derivation of the electronic coupling from experimental ET rate data. This method avoids direct calculation of the transfer integral by assuming the validity of Marcus' ET rate equation and suitably modeling the water medium.

In the present work, we perform a direct many-electron calculation of the transfer integral, within the DFT scheme, using several solvent configurations sampled from ab initio molecular dynamics (MD) simulations. This allows exploration of the non-Condon effects related to the dynamical nature of the water medium and a reliable estimate of the root-mean-square transfer integral to be inserted into Marcus' equation for the ET rate constant. The DFT scheme treats the electronic correlation effects in the presence of metal ions and offers the best compromise between accuracy and feasibility in the study of complicated systems involving the redox couple $Fe^{2+}-Fe^{3+}$ (e.g., in the presence of mineral surfaces and contaminants). The formula[23] adopted to compute the electronic couplings does not resort to empirical parameters, require knowledge of the exact transition-state coordinate, and make use of excited-state quantities. However, the approximate character of any currently available exchange-correlation functional (leading to spurious self-interaction terms in the energy) along with the complicated electronic structure of the transition-metal system under consideration requires the use of the abovementioned formula in a suitable FON-DFT scheme and a remedy for self-interaction errors. In the present context, such errors are corrected to the level allowed by DFT + U[28] electronic structure calculations, while the effects related to the nondynamical electron correlation[29] are coped with via a suitable FON approach.

The work is organized as follows. Section 2 deals with the theory. In section 2.1 we introduce the model system on which the ab initio calculations are performed. Section 2.2 briefly reviews Marcus' equation for the ET rate constant and the adopted formula[23] for transfer integral evaluation. The general issue of the problematic self-consistent field calculations in transition-metal systems is addressed in section 2.3. This is followed by analysis (sections 2.4 and 2.5, Appendix B, and Supporting Information) of the FON-DFT scheme for values of the smearing parameter well beyond those studied in previous works. We identify and rationalize a linear regime (and a wider range of approximately linear behavior) of energy eigenvalues, chemical potential, and FON entropic term. Our theoretical analysis provides a recipe for an appropriate choice of the broadening parameter in calculating transfer integrals. The main computational results and their analysis are presented in section 3: Computational details are reported in section 3.1. The ab initio transfer integral calculations, with and without the Hubbard U correction scheme (introduced to improve the description of the electronic charge distribution), for selected nuclear configurations are presented in section 3.2. They are compared with the couplings obtained by the pathway model[16] in section 3.3 and with the experimental expectations in section 3.4. In particular, the ab initio root-mean-square electronic coupling is combined with prior theoretical estimates of the reorganization energy[30,31] to get a fully ab initio value of the electron self-exchange rate. Finally, the calculated and observed[32] rates are compared, and Marcus' equation for the concerned ET rate is assessed. Analytical details of the theoretical development on FON-DFT achieved in this work and used to compute the transfer integrals are presented in Appendix B (and Supporting Information) after an overview of the standard FON-DFT Scheme with Gaussian Broadening in Appendix A. The Hubbard U correction to DFT is detailed in Appendix C.

2. Theory

2.1. Model Redox System. The redox system under consideration is $Fe_{aq}^{2+}-Fe_{aq}^{3+}$. In this paper attention is focused on the solvation cages since the effects of the outside water on the electronic coupling can be considered relatively minor[3,15] (also based on general considerations about the tunneling nature of the electronic coupling between redox partners[21]). The nonadiabatic electron self-exchange reaction under study is

$$Fe(H_2O)_6^{2+} - Fe(H_2O)_6^{3+} \rightarrow Fe(H_2O)_6^{3+} - Fe(H_2O)_6^{2+} \quad (1)$$

where the electron-transfer process leads to the formation of the successor complex (right side) from the precursor complex (left side). The two groups are the localized donor (D) and acceptor (A) species, whose structural identity is maintained throughout the (outer-sphere) reaction.[15] The D and A groups are assumed to be in contact around the transition state, at the ET optimal interionic distance of 5.5 Å,[3−5,33] also adopted in the MD simulations of ref 30.

2.2. ET Rate and Transfer Integrals. In the present work we deal with the rate of the ET process (once the transition state is reached) as controlled by the magnitude of the transfer integral. For nonadiabatic ET reactions, which are characterized by a weak electronic coupling between the D and A groups, the rate constant is approximately given by the high-temperature expression

$$k_{ET} = \sqrt{\frac{\pi}{\lambda k_B T}} \frac{\langle V_{IF}^2 \rangle}{\hbar} \exp\left[-\frac{(\Delta G^\circ + \lambda)^2}{4\lambda k_B T}\right] \quad (2)$$

where λ is the reorganization energy, $\Delta G°$ is the reaction free energy (in particular, it is zero for a self-exchange reaction), k_B is Boltzmann's constant, T is the temperature, $\langle V_{IF}^2 \rangle$ is the mean-square value of the transfer integral, which measures the coupling between the initial state I and the final state F of the ET reaction. The average in eq 2 expresses a "relaxed" Condon approximation, which holds in the limit of slow modulation of the ET rate by the nuclear motion[34] and captures the average effects of the changes in the water configuration. In fact (see Supporting Information), even if the Condon approximation does not hold (because of a significant dependence of the transfer integral on the arrangement of the water molecules), its "relaxed" form appropriately accounts for the effects of the electronic coupling on the ET rate due to the actual uncoupling of nuclear and electronic motions.

The averaging on the transfer integral in eq 2, as performed in our calculations, is strictly related to the distinction between accepting modes and inducing modes.[34] The first ones support the energy exchanges necessary both to make the relevant donor and acceptor levels nearly degenerate in energy and to relax the nuclear structure after the electron transition occurs. Along these modes ET can happen only for a regime of configurations near the transition state, so that the Condon approximation can be applied. Indeed, the reaction coordinate depends on the overall set of accepting modes. The inducing modes are weakly coupled to the D and A states, so that the electron transfer is not limited to a small range of configurations along them. In fact, the effects of the disordered water motion can be negligible on the energies of the localized (*diabatic*) D and A electronic states while considerable and probably fluctuating on the coupling between such states. Our implementation of eq 2 can be depicted in terms of a two-dimensional space of the water nuclear configurations, spanned by a reaction coordinate and an orthogonal inducing coordinate.[35] The MD simulations from ref 30 exploited in this work allow a mapping onto the aforementioned space, and the transfer integral is computed on sampled configurations around the reaction coordinate of the transition state. Hence, variable magnitudes necessarily arise from distinct points along the inducing coordinate.

The ab initio computation of the transfer integrals is performed by means of the formula[23]

$$V_{IF} = \left| \frac{\Delta E_{IF} ab}{a^2 - b^2} \right| \tag{3}$$

where ΔE_{IF} is the energy difference between the ET diabatic states I and F, and a and b are their respective overlaps with the ground state of the system. The initial state vector is defined as $|\psi_I\rangle = |D\rangle|A\rangle$ and the final state vector as $|\psi_F\rangle = |D^+\rangle|A^-\rangle$, where $|D\rangle$ ($|D^+\rangle$) denotes the reduced (oxidized) ground state of the isolated donor site and $|A^-\rangle$ ($|A\rangle$) the reduced (oxidized) ground state of the isolated acceptor site. Therefore, in the two-state model the ground-state vector of the system is given by $|\psi\rangle = a|\psi_I\rangle + b|\psi_F\rangle$. The approximations involved in eq 3 and the feasibility of appropriately using DFT wave functions are detailed in ref 23, where it is also stressed that it yields a dependence of the electronic coupling on the distance between the redox centers in good agreement with the empirical average packing density model.[36] Moreover, within the theoretical framework of ref 23 eq 3 gives the best estimate of the transfer integral also when the two-state approximation is not satisfied. The quantity ΔE_{IF} is given by

$$\Delta E_{IF} = (E_D + E_A) - (E_{D^+} + E_{A^-}) + W_{D-A} - W_{D^+-A^-} \tag{4}$$

where E_D (E_{D^+}) is the ground-state energy of the isolated donor group in its reduced (oxidized) state of charge, E_A (E_{A^-}) is the same for the acceptor group in its oxidized (reduced) state, $W_{D\text{-}A}$ and $W_{D^+\text{-}A^-}$ are the energies of (essentially electrostatic) interaction between the D and A groups in the initial and final diabatic states, respectively.

2.3. Problematic SCF Convergence. Equation 3 has been implemented into a spin-polarized DFT scheme. In this section we show that self-consistent field (SCF) calculations, in the absence of fractional occupations of the Kohn−Sham (KS) spin orbitals, hardly manage to converge. Moreover, the convergence, if it is achieved, generally leads to a dramatic failure in the description of the electronic ground state with the transferring electron charge abnormally shared between the two iron centers.[30,37]

The issue of the troublesome SCF convergence can be well appreciated starting from the effective one-particle KS equations. In atomic units they are written as[38]

$$H([n_s], \mathbf{r})\psi_i(\mathbf{r}) \equiv \left[-\frac{1}{2}\nabla^2 + V_H([n_s], \mathbf{r}) + v_{xc}([n_s], \mathbf{r}) \right] \psi_i(\mathbf{r}) = \varepsilon_{si}\psi_i(\mathbf{r}) \tag{5}$$

where $i = 1$ to N, N is the total number of electrons, H denotes the KS Hamiltonian operator, $n_s(\mathbf{r})$ is the ground-state density of the auxiliary system of noninteracting electrons (which equals the exact density of the interacting system), V_H is the Hartree potential, v_{xc} is the exchange-correlation (XC) potential, ψ_i is the ith spin orbital, and ε_{si} is the corresponding energy eigenvalue.[39] Equation 5 is to be solved in a self-consistent manner under the constraint $n_s(\mathbf{r}) = \sum_{i=1}^{N} |\psi_i(\mathbf{r})|^2$, which expresses the ground-state density in terms of the N lowest KS spin orbitals. Due to the approximate character of any currently available XC functional the iterative solution of eq 5 leads to incorrect wave functions (φ_i), energy eigenvalues (ε_i), and density (n), which satisfy the approximate equations

$$H^{approx}([n], \mathbf{r})\varphi_i(\mathbf{r}) \equiv \left[-\frac{1}{2}\nabla^2 + V_H([n], \mathbf{r}) + v_{xc}^{approx}([n], \mathbf{r}) \right] \varphi_i(\mathbf{r}) = \varepsilon_i\varphi_i(\mathbf{r}) \tag{6}$$

where $n(\mathbf{r}) = \sum_{i=1}^{N} |\varphi_i(\mathbf{r})|^2$ is the electron density and v_{xc}^{approx} the approximate XC potential. By considering the operators into eqs 5 and 6 after the respective self-consistency is achieved we recast eq 6 in the form

$$(H([n_s], \mathbf{r}) + W([n], [n_s], \mathbf{r}))\varphi_i(\mathbf{r}) = \varepsilon_i\varphi_i(\mathbf{r}) \tag{7}$$

with

$$W([n], [n_s], \mathbf{r}) = (V_H + v_{xc})([n], \mathbf{r}) - (V_H + v_{xc})([n_s], \mathbf{r}) + v_{xc}^{approx}([n], \mathbf{r}) - v_{xc}([n], \mathbf{r}) \tag{8}$$

Equation 8 displays two different, although related, contributions to W. The former comes from the difference in the

total potential, with the correct functional form, evaluated on the approximate and exact charge densities. The latter is due to the incorrect functional form of v_{xc}. It persists even if n happens to be so close to n_s that the first contribution can be neglected.

By applying the stationary perturbation theory[40] to eq 7 we get the following connection between the exact and the approximate KS spin orbitals in terms of the "perturbation" W (i.e., the deviation from the exact one-particle Hamiltonian)

$$\varphi_i(\mathbf{r}) = \psi_i(\mathbf{r}) + \sum_{n \neq i} \frac{\langle \psi_n | W | \psi_i \rangle}{\varepsilon_{si} - \varepsilon_{sn}} \psi_n(\mathbf{r}) + O(W^2) \qquad (9)$$

According to eq 9, the departure of φ_i from the corresponding wave function ψ_i (i.e., the spin orbital coming from the use of the exact XC potential) is determined by the mixing of ψ_i with the other orbitals ψ_n ($n \neq i$) through W. The closer the KS energy levels ε_{si} and ε_{sn} and the stronger the coupling $\langle \psi_n | W | \psi_i \rangle$, the larger the mixing between ψ_i and ψ_n. Therefore, the approximate character of the XC potential can affect (sometimes to a great extent) the shapes of the wave functions and thus the values of the overlap parameters a and b entering on eq 3. In this respect, a crucial source of errors is the unphysical self-interaction of the relevant electronic charge with itself arising from the fact that the approximations to the XC energy are independent of the electrostatic repulsion term.

In the presence of open-shell atoms a further complication stems from the multiplet problem since the currently available XC functionals do not have the appropriate spin and spatial symmetry behavior to correctly describe multiplet systems.[41] Such a problem is exacerbated in the case that molecular orbitals centered on different redox sites come to be virtually degenerate. One way out consists of the use of a linear combination of determinants to describe the wave function of the system.[41]

Finally, a computational issue (possibly related to the previous ones in a DFT scheme) comes out by considering eq 9 (and the equations which express the second-order correction to the energy as well as higher terms in both the energy and the spin−orbital perturbation expansions) over a SCF calculation. In fact, as the potential (initially corresponding to the wrong guess density) is changed between subsequent iterations to move toward the self-consistency, a computational contribution to W intervenes to mix the spin orbitals. On one hand, this is an intrinsic feature of the iterative procedure, exploitable to obtain quadratic SCF convergence.[42] On the other hand, it cannot be used effectively when the gap between the highest occupied molecular orbital (HOMO) and the lowest unoccupied molecular orbital (LUMO) is particularly small. Rather, in such a case, the convergence is generally problematic and can lead to unstable solutions, all the more that a small HOMO−LUMO gap is often accompanied by a high density of states near the Fermi energy, defined as the average of the HOMO and LUMO energies for finite systems with integral occupation numbers.[42] Indeed, it has been formally shown, within the HF scheme, that SCF convergence is slowed by a small gap at the Fermi energy.[43] In general, oscillations in the iterative solution of one-electron equations arise whenever some orbitals close to the Fermi level are alternatively occupied and unoccupied from one iteration to the next. One way to damp these oscillations consists in allowing fractional occupations.[44]

In the ferrous−ferric system the generally asymmetric arrangement of the aqueous environment around the two ions moves the ground state out of degeneracy. Therefore, a single-determinant picture of the ground-state wave function is allowed. However, the levels corresponding to some d-like molecular orbitals preserve a multiplet structure. This can be envisaged by taking jointly into account the near degeneracy of the atomic d orbitals and the fact that close enough to the transition state one-half of the gap between the HOMO and LUMO levels are comparable with the expected value of the transfer integral.[22,45] In particular, the HOMO and the LUMO, each expected to be essentially localized on a different ion (although with a tail onto the other ion, owing to the electronic coupling between the two redox sites), correspond to very similar energies for all of the sampled nuclear configurations. Hence, due to the abovementioned computational issues, DFT calculations without fractional occupation numbers, when they manage to convergence, almost always lead to a quite inaccurate HOMO, which is a linear combination of the correct HOMO and LUMO exceedingly spread over the two sites. Thus, the ground-state wave function, obtained as a Slater determinant of the lowest occupied orbitals, is unduly delocalized over the D and A groups and the overlaps a and b entering on eq 3 are correspondingly similar, leading to anomalously large values of the transfer integral. This behavior is illustrated in Figure 1. It shows that the value of the transfer integral diverges when the electron smearing becomes so small that all the molecular orbitals have integral occupation numbers. Moreover, for several other nuclear configurations SCF convergence without FON has been not achieved.

It is worth noting that, while the interplay between the computational issues and the approximations incidental to the DFT scheme is in general responsible for an almost equal spread of the HOMO (which describes the ET system in the one-electron picture and is the crucial orbital in determining the transfer integral also in the multielectron picture[12,15]) over the two redox centers, the spurious electronic self-interaction is, by itself, sufficient for a considerable overestimation of the electronic coupling. In fact, the latter is crucially dependent on the small tail of the HOMO, which can be drastically affected by self-interaction errors, even if they cause a negligible relative change in the correct charge density around the ion where the spin orbital is prominently localized.

In this work, the electron-smearing technique proposed by ref 46 (where a broadening parameter is used to get the SCF convergence and then gradually reduced to zero) has been successfully used for some calculations on the isolated redox groups, necessary to derive the localized wave functions ψ_I and ψ_F, while it turned out not to work in the presence of both ions. For the electronic structure calculations on the overall system we use an alternative approach. Fractional occupations are suitably exploited to get the convergence. Then the spin orbitals up to the nominal HOMO are used to build the necessary wave

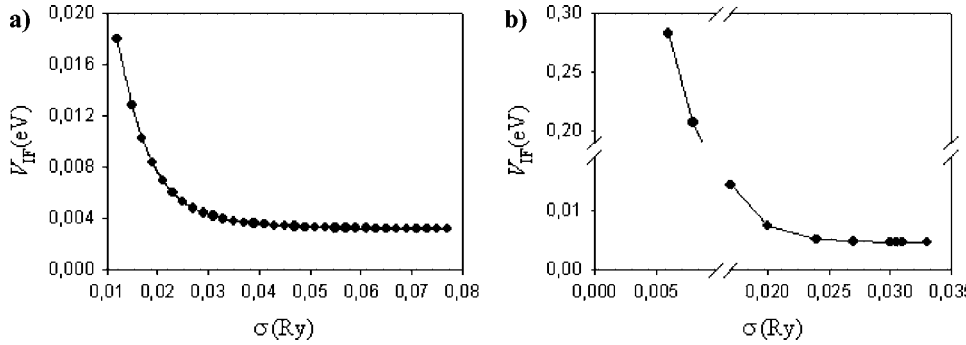

Figure 1. Transfer integrals by eq 3 vs spreading parameter σ for the Gaussian broadening of the orbital occupation numbers (see below). The panels correspond to different nuclear configurations taken from a Car−Parrinello molecular dynamics (CPMD) run in ref 30 after (a) 9000 and (b) 24 000 steps. Each time step is 5 au. The overall production run lasts 60 000 steps.

functions, while the virtual spin orbitals with "fake" occupation are disregarded.[47] With reference to eq 3, where only the ground-state wave function of the overall system is employed, the latter procedure requires that the orbital relaxation exclusively due to the smearing of the electron charge (once the abnormal spreading of the HOMO is avoided) is negligible. This is in analogy with the approximation on relaxation pertaining to Koopmans' theorem (in both the HF[48] and DFT[49] schemes), although that theorem involves an integer change of the LUMO occupation with a corresponding increase in the net electronic charge. On the other hand, the analogy cannot be pushed far enough to justify the employed approach, which requires a specific theoretical basis. The pertinent analysis (sections 2.4 and 2.5, Appendix B, and Supporting Information) is also essential to identify the appropriate values of the smearing parameter to be used in transfer integral evaluation.

From an analytical point of view we note that in the presence of fractional occupations f_i of the orbitals eq 6 turns into

$$\left[-\frac{1}{2}\nabla^2 + v_{\text{eff}}([n_\sigma],\mathbf{r})\right]\varphi_i(\mathbf{r};\sigma) = \varepsilon_i(\sigma)\varphi_i(\mathbf{r};\sigma) \qquad (10)$$

where $v_{\text{eff}}([n_\sigma],\mathbf{r}) \equiv v_{\text{eff}}(\mathbf{r};\sigma) = V_{\text{H}}([n_\sigma],\mathbf{r}) + v_{\text{xc}}^{\text{approx}}([n_\sigma],\mathbf{r})$ is the effective single-particle potential and n_σ is the electronic charge density given by

$$n_\sigma(\mathbf{r}) \equiv n(\mathbf{r};\sigma) = \sum_{i=1}^{N} f_i(\sigma)|\varphi_i(\mathbf{r};\sigma)|^2 \qquad (11)$$

The Hamiltonian operators in eqs 6 and 10 differ by the term $v_{\text{eff}}([n_\sigma],\mathbf{r}) - v_{\text{eff}}([n],\mathbf{r})$. In section 2.5 we show that this difference, stemming from the FON approach, can only lead to minor changes in the orbitals when a suitable SCF convergence can be achieved also for a vanishing electron smearing. Thus, the orbitals derived by means of the FON-DFT approach can only suffer significantly from the intrinsic approximations of v_{eff}, that is, mainly from self-interaction errors. We will take care of the latter by the method illustrated in Appendix C, which also allows calculation of the transfer integral without fractional occupations for some of the considered nuclear configurations.

2.4. Single-Particle Energies, Chemical Potential, and Energy Terms in the Gaussian FON-DFT Scheme. For all the sampled configurations of the water medium the computed electronic structure of the aqueous ferrous−ferric

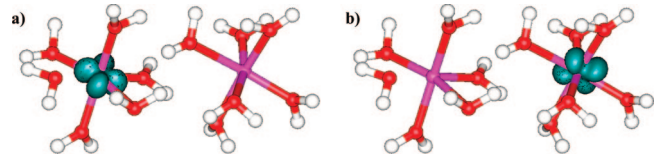

Figure 2. Minority-spin (a) HOMO and (b) LUMO for the configuration after 24 000 simulation steps. The small tail of each orbital on the other redox center (for the HOMO it is due to the nonzero transfer integral) is not visible at the represented isovalue of 0.02.

system (in its high-spin state) turns out to be characterized by a multiplet of levels ε_j ($j = 1,..., N_d$), which correspond to minority-spin orbitals with a predominant d-like character. For instance, Figure 2 displays the two lowest d-like MOs for one of the selected configurations. The remaining MOs in the multiplet have a similar shape (i.e., they are essentially d type orbitals of t_{2g} symmetry), dictated by the electrostatic field of the solvation water. In fact, we always obtain $N_d = 6$. Instead, the atomic 4s orbital and the other atomic 3d orbitals give rise to higher virtual levels well separated from the multiplet.

In fact, the half-width of the d-like multiplet turns out to be within ca. 0.25 eV for all of the selected nuclear configurations, whereas the separation between the mean energy of the multiplet and the higher lying levels is always above 1 eV and the lower lying levels are at least 2 eV far apart. Such a level structure allows a relatively wide range of σ values larger than the spreading of the d-like multiplet and smaller than the separation from the remaining levels, which are denoted by ε_k. In the present section we exploit this feature, common to many other open-shell transition-metal systems, and develop the formalism of the FON-DFT approach with Gaussian broadening in order to obtain useful connections between the KS single-particle energies, the chemical potential, and the entropy. The resultant analysis provides the theoretical justification for the derivation of the ground-state wave function from the FON-DFT approach, whereas the corresponding electronic density is not used.

For the aforementioned values of σ, by analytical elaboration of eq 27 of Appendix A and exploitation of Cardano's formula,[50] we obtain (see Supporting Information)

$$\varepsilon_j(\sigma) - \mu(\sigma) = [A(N_d) + B(N_d)\omega_j(\sigma)]\sigma \qquad (12)$$

where the deviation numbers

$$\omega_j(\sigma) = f_j(\sigma) - \frac{1}{N_d} \tag{13}$$

measure the departure from an even occupation of the MOs in the multiplet. For $N_d = 6$, the numerical values of A and B are 0.57 and −1.57, respectively. Moreover, the dependence of B on N_d is negligible. The addition of eq 12 corresponding to the different ε_j and the requirement that the deviation numbers add up to zero (as long as the fractional occupations f_j add up to unity) yield the following useful connection between the chemical potential and the mean energy $\langle\varepsilon(\sigma)\rangle$ of the multiplet

$$\mu(\sigma) = \langle\varepsilon(\sigma)\rangle - A(N_d)\sigma \tag{14}$$

If $\langle\varepsilon(\sigma)\rangle$ is approximately independent of σ, as the levels ε_j mix among them,[51] and σ is sufficiently large for the validity of eq 14, then the chemical potential has a linear dependence on σ. As exemplified by Figure 3, this is the case in a wide range of σ values. Moreover, the slope of the dashed line in Figure 3b is 0.58, which is very close to the value 0.57 predicted by eq 14 for $N_d = 6$.

When σ becomes comparable with the energy gap between the d-like multiplet and the other levels, $\langle\varepsilon(\sigma)\rangle$ changes appreciably (e.g., see Figure 3a) and μ is no longer a linear function of σ. The energy gap below the multiplet is wider than the one above it. However, the spreading of the transferring electron over the multiplet determines a decrease of the chemical potential, which gets closer to the lower lying levels and increasingly smaller than the mean energy of the multiplet. On the whole, at the upper edge of any explored σ range the deviations of the lower lying levels from unit occupation are small (less than 0.05) and comparable with the deviations of the higher lying levels from zero occupation. Therefore, μ levels off beyond the linear regime (see Figure 3b). On the other hand, the smaller energy gap above the multiplet determines a stronger mixing between the latter and the higher virtual levels. This causes the increase of $\langle\varepsilon\rangle$ illustrated by Figure 3a. We conclude that although the chemical potential is an even function of σ when the electron density does,[52] its behavior can be linearized in a suitable (wide) range of the broadening parameter.

When σ is much larger than the spreading of the d-like multiplet, while still small relative to the gap with the higher KS levels (i.e., for σ well inside the range of values where the chemical potential has a linear behavior, referred to as the *linear regime*), the levels ε_j get almost equally occupied so that $f_j \approx 1/N_d$ and $\omega_j \approx 0$. This is to say that in the asymptotic expansion of ω_j around any of such σ values

$$\omega_j(\sigma) = \omega_{0j} + \frac{\omega_{1j}}{\sigma} + \cdots \tag{15}$$

the zero-order term is quite small and $\omega_{1j} \ll \sigma$. More generally, in the σ range where the expansions of eq 15 can be truncated to the first order in $1/\sigma$, their insertion into eq 12 gives

$$\varepsilon_j(\sigma) - \mu(\sigma) = [x_j(\sigma) + A(N_d)]\sigma = B\omega_{1j} + [B\omega_{0j} + A(N_d)]\sigma \tag{16}$$

Equation 16 predicts the behavior of the relative energies $\varepsilon_j - \mu$ in the linear regime and is closely confirmed by the computational results (see Supporting Information). It is also worth noting that the slopes of the curves represented by eq 16 are quite similar since A is much larger than $B\omega_{0j}$.

For values of the Gaussian broadening beyond the linear regime the orbitals corresponding to out-of-multiplet levels (ε_k) begin to have appreciable fractional occupations. Since all the levels ε_j correspond to d-like MOs and are very close in energy relative to the remaining levels ε_k, they mix to a similar amount with the latter (as can be seen by means of the stationary perturbation theory, accomplished up to second-order corrections[53]). As a consequence, beyond the linear regime the levels ε_j do not branch off. Rather, they continue to experience an almost identical shift as functions of σ. More specifically, in the Supporting Information we describe the behavior of the KS relative energies for values of σ beyond the linear regime, although still corresponding to the plateau of the transfer integral (that is, according to eq 3, corresponding to a negligible orbital relaxation).

As shown in the Supporting Information, the linear regime is also characteristic of the behavior of the entropic contribution $-\sigma S(\sigma)$ to the fictitious free energy. In fact, it is

$$S(\sigma) = \frac{N_d}{2\sqrt{\pi}}\exp(-A^2)\left[1 + \frac{2A^2-1}{N_d}\sum_j\left(B^2\omega_{0j}^2 + \frac{2B^2\omega_{0j}\omega_{1j}}{\sigma} + \cdots\right)\right] \cong S_0 - \frac{S_1}{\sigma} \tag{17}$$

where the positive coefficients S_0 and S_1 are introduced, the sum is restricted to the levels ε_j (which is appropriate in the linear regime, where the levels ε_k are still empty), and the terms up to the first order in $1/\sigma$ are retained in the last

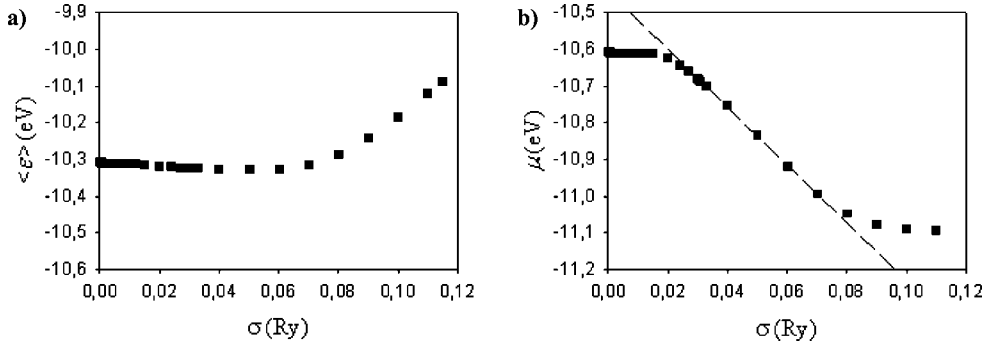

Figure 3. (a) $\langle\varepsilon\rangle$ vs σ and (b) μ vs σ for the nuclear configuration after 24 000 simulation steps. The vertical axis is translated upward in the b panel. The dashed line fits to the data points in the linear region of the entropic term (see below).

approximate expression. By considering the relation[52] $dE/d\sigma = \sigma(dS/d\sigma)$, eq 17 yields the following expression for the energy

$$E(\sigma) = E(\sigma_0) + S_1 \ln \frac{\sigma}{\sigma_0} \tag{18}$$

Finally, from eqs 17 and 18 we obtain the fictitious free energy

$$F(\sigma) = E(\sigma_0) + S_1 \ln\left(e\frac{\sigma}{\sigma_0}\right) - S_0\sigma \tag{19}$$

Equations 17, 18, and 19 describe the behavior of the FON-DFT entropy, energy, and free energy in a wide range of σ, starting from a value σ_0 at the onset of the linear regime. Therefore, they are complementary to the power series (up to the second order in σ) in eqs B4 and B5 of ref 52, which are valid for small enough σ. Equation 11 of ref 52 shows that $1/2[F(\sigma)+E(\sigma)] = E(0) + O(\sigma^n)$ with $n > 2$, thus providing a method to calculate the correct energy (without electron smearing) from the results at a suitably small σ. In this work the value of n is not found, but eqs 18 and 19 clearly show that such a method cannot be used in the linear regime. Furthermore, as shown in next section, eq 18 yields a sufficient condition for suitably picking the value of σ in the calculation of the transfer integral.

2.5. Single-Particle Quantities and Orbital Relaxation Analysis: An Alternative Approach to FON-DFT. In section 2.4 we showed that the KS levels experience almost identical shifts in a large σ range, with approximately equal slopes. In particular, the value of the transfer integral is always picked in correspondence to a σ in the linear regime, although the relative changes of the transfer integral are negligible also beyond such a regime. Indeed, there is a strict connection between the regime of nearly uniform behavior of the single-particle energies and the orbital relaxation. In the HF scheme the shape and the energy of an orbital are independent of its occupation number if the remaining orbitals do not relax.[54] This circumstance does not occur in any DFT calculations due to the spurious electron self-interaction. However, as stressed in ref 55 within the context of Janak's theorem, when orbital relaxation is negligible a substantial linear response (i.e., the orbital energy is a linear function of the occupation number) can be expected in the presence of the electron self-interaction. Moreover, in refs 49 and 56(with particular reference to the DFT Koopmans' theorem in large molecular systems) it is noted that orbital relaxation can be appraised by the nonuniformity of the KS level shift.

In this section (see also Appendix B) we present a theoretical analysis which provides a general connection between the Gaussian broadening and the orbital relaxation as mediated by the KS effective potential and is able to circumscribe the errors that can arise when the orbital relaxation is completely ignored. The latter point is particularly important when dealing with ET between small complexes. It is also worth noting that the provided formalism can be directly applied to other electron-transfer systems (e.g., electron self-exchange reactions, where the HOMO and the LUMO are characterized by the same quantum numbers). The two main goals of the approach, as for the evaluation of the transfer integrals, are as follows: (i) theoretical proof that the relaxation of the spin orbitals is negligible in the entire large σ range, so that a stable value of the transfer integral can be derived from them; (ii) analytical assessment that such orbitals, denoted by $\bar{\varphi}_i(\mathbf{r};\sigma)$, are an adequate approximation to the computationally inaccessible orbitals in the absence of the occupation Gaussian broadening, denoted by $\varphi_i(\mathbf{r};0)$, so that the corresponding value of the transfer integral is reliable.

A general equation, which transparently discloses the connection between $\bar{\varphi}_i(\mathbf{r};\sigma)$ and $\varphi_i(\mathbf{r};0)$, owing to the dependence of the KS effective potential v_{eff} on σ, can be derived by exploiting the formalism of the quantum theory of scattering by a potential. In fact, the Kohn−Sham equations, after self-consistency is achieved, can be written as

$$\left[-\frac{1}{2}\nabla^2 - \varepsilon_i(0) + v_{\text{eff}}(\mathbf{r};0)\right]\bar{\varphi}_i(\mathbf{r};\sigma) = [\Delta\varepsilon_i(\sigma) - \Delta v_{\text{eff}}(\mathbf{r};\sigma)]\bar{\varphi}_i(\mathbf{r};\sigma) \tag{20}$$

where

$$\Delta\varepsilon_i(\sigma) = \varepsilon_i(\sigma) - \varepsilon_i(0) \tag{21a}$$

$$\Delta v_{\text{eff}}(\mathbf{r};\sigma) = v_{\text{eff}}(\mathbf{r};\sigma) - v_{\text{eff}}(\mathbf{r};0) \tag{21b}$$

and $\Delta\varepsilon_i - \Delta v_{\text{eff}}$ works as a "scattering potential". The solution of the homogeneous equation associated to eq 20 is just $\phi_i(\mathbf{r};0)$, while the Green's function of the pertaining operator, that is the solution of the equation

$$\left[-\frac{1}{2}\nabla^2 - \varepsilon_i(0) + v_{\text{eff}}(\mathbf{r};0)\right]G_i(\mathbf{r}) = \delta(\mathbf{r}) \tag{22}$$

is

$$G_i(\mathbf{r}) = \frac{1}{2\pi r}\frac{\varphi_i(\mathbf{r};0)}{\varphi_i(\mathbf{0};0)} \tag{23}$$

The origin of the coordinate reference system can be arbitrarily chosen wherever the denominator of eq 23 is not null. From eqs 20, 21a, 21b, 22, and 23 it is seen that the wave function $\bar{\varphi}_i(\mathbf{r};\sigma)$ fulfills the integral "scattering" equation

$$\bar{\varphi}_i(\mathbf{r};\sigma) = \varphi_i(\mathbf{r};0) + \frac{1}{2\pi\varphi_i(\mathbf{0};0)}\int d^3r', \frac{\varphi_i(\mathbf{r}-\mathbf{r'};0)}{|\mathbf{r}-\mathbf{r'}|} \times [\Delta\varepsilon_i(\sigma) - \Delta v_{\text{eff}}(\mathbf{r'};\sigma)]\bar{\varphi}_i(\mathbf{r'};\sigma) \tag{24}$$

Equation 24 illustrates the role played by $\Delta v_{\text{eff}}(\mathbf{r};\sigma)$ (i.e., the change in the KS effective potential due to the Gaussian broadening) in the rearrangement of the orbitals. The theoretical analysis of eq 24, illustrated in Appendix B, shows that the integral term, owing to the "scattering potential" and mixing the correct spin orbitals, can be neglected at any σ within a suitable range, which includes all the linear regime. In particular, this holds for the HOMO, which is the crucial spin orbital in the calculation of the parameters a and b in eq 3, and thus of the effective electronic coupling.

Once demonstrating the reliability of the transfer integral evaluation in the plateau region, the sufficient condition represented by the fulfillment of eq 18 provides a useful computational tool, as the exploration of the σ range can be

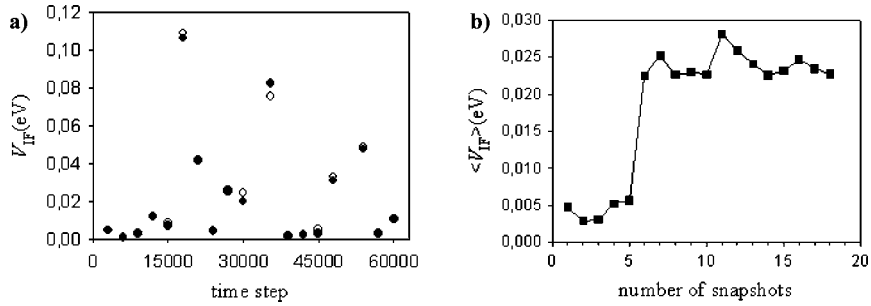

Figure 4. (a) Effective electronic coupling vs CPMD step number for the PW91-GGA (○) and PBE-GGA (●) calculations. (b) Dependence of the PBE-GGA mean transfer integral on the number of configurations used to compute the average.

stopped when the onset of the linear regime is detected. Ultimately, we also note that the nearly even occupation of the d-like MOs well inside the plateau region (where the coupling is obtained) can be regarded as an extension of the Slater transition-state notion[57] (but see the discussion in p 58 of ref 38 about the definition of the transition-state density).

Note that the theoretical analysis in this section and Appendix B adequately delimits the errors arising from the Gaussian spreading of the electron charge, which is responsible for a change $\Delta v_{\text{eff}}(\mathbf{r};\sigma)$ in the KS effective potential, whereas it does not envisage the errors in both $v_{\text{eff}}(\mathbf{r};\sigma)$ and $v_{\text{eff}}(\mathbf{r};0)$ resulting from the spurious electronic self-interaction. The computational achievement of a plateau of the transfer integral over a wide range of σ, where occupation of the HOMO changes by a significant fraction of the electron charge e (e.g., from $0.2e$ to more than $0.3e$ for the cases depicted in Figure 1), indicates that $v_{\text{eff}}(\mathbf{r};\sigma)$ and $v_{\text{eff}}(\mathbf{r};0)$ are affected by similar self-interaction errors. The recipe used for self-interaction correction (SIC), thus yielding a FON-DFT + U approach, is described in Appendix C.

3. Computation

3.1. Computational Details. The transfer integrals are computed through eqs 3 and 4, on the system of eq 1, for selected nuclear configurations along a Car−Parrinello MD[58] (CPMD) run taken from ref 30. The CPMD time step is 5 au, and the selected snapshots are 3000 steps apart (∼0.36 ps). The required electronic properties are computed by means of the PWscf code,[59] in the repeated supercell approach, by using the plane-wave spin-polarized DFT scheme in both the Perdew−Wang[60] (PW91) and the Perdew−Burke−Ernzerhof[61] (PBE) generalized gradient approximation (GGA). The DFT + U method is applied with the PBE exchange-correlation functional. The wave function and charge density cutoffs are 25 and 200 Ry, respectively. The atomic cores are represented by ultrasoft pseudopotentials from the standard QUANTUM-ESPRESSO distribution[59] (specifically, H.pw91-van_ak.UPF, O.pw91-van_ak-.UPF, and Fe.pw91-sp-van_ak.UPF for the PW91 exchange-correlation functional; H.pbe-rrkjus.UPF, O.pbe-rrkjus.UPF, and Fe.pbe-sp-van_mit.UPF for the PBE functional). The Fe pseudopotential corresponds to 16 valence electrons. The size of the repeating cell is $15 \times 15 \times 20$ Å^3 (20 Å along the direction of the irons). Calculations with large values of σ are performed by constraining the total magnetization in such a way that the total numbers of the majority-spin and minority-spin electrons are fixed, and the system is strictly preserved in the correct high-spin state (which is used in ref 30; see also refs 3 and 62).

The relevant wave functions are constructed as single Slater determinants of the lowest lying KS spin orbitals up to the nominal HOMO (which is a true HOMO for the single-site wave functions, obtained without fractional occupations). The feasibility of using DFT wave functions is argued in ref 23 and references therein. The overlaps between the spin orbitals, necessary to derive the overlap integrals a and b into eq 3, are computed through the DTI program.[63] The interactions in eq 3 ($W_{\text{D-A}}$ and $W_{\text{D}^+\text{-A}^-}$) are obtained by full electrostatics calculations exploiting the Poisson equation and the electrostatic potential provided by the PWscf program.

In the (FON-)DFT + U approach the U parameter is computed through the PWscf code. The same U is used for obtaining the electronic structures of the isolated donor and acceptor groups (in the oxidation states corresponding to the initial and final ET states) and of the whole system, which are required by eq 3. The dependence of the electronic charge distribution and thus of the electronic correlation on nuclear coordinates is taken into account by separately evaluating the U interaction parameter for each selected configuration.

3.2. Tranfer Integrals. The couplings computed through the spin-polarized FON-DFT approach in the PW91-GGA and the PBE-GGA are represented in Figure 4a. For each point a plateau of the transfer integral (as in Figure 1) has been obtained. The changes along the plateaus are generally nonmonotonic, amount to less than 5%, and are mainly attributable to the shortcomings of the two-state model. For any nuclear configuration the choice of the σ value (within the respective plateau) for evaluation of the electronic coupling is essentially arbitrary due to the small relative error. Anyhow, the adopted criterion lies in the use of the σ value which yields the maximum localization of the nominal HOMO on one of the ET sites and thus the smallest electronic coupling. This choice opposes the overestimation of the coupling by any DFT scheme without full self-interaction correction and corresponds to the maximum (nominal) HOMO−LUMO gap. The latter circumstance matches the fact that any SIC approach tends to enlarge that gap (e.g., this can be seen from the expressions of the single-particle energies in the Perdew−Zunger SIC scheme[64]).

As shown in Figure 4a, PW91-GGA and PBE-GGA give very similar results. This matching is generally expected,

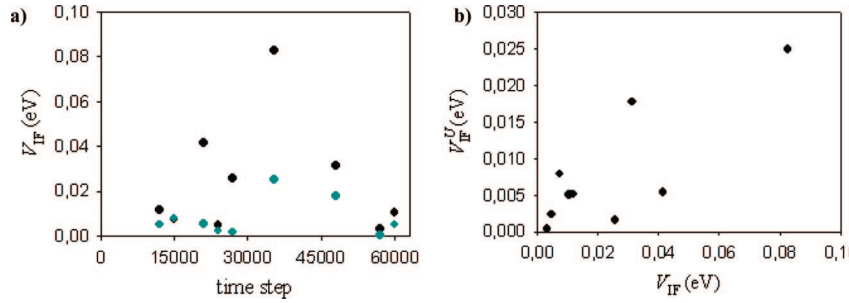

Figure 5. (a) Transfer integral vs CPMD step number. The dark circles represent the transfer integrals by the FON-DFT approach with the PBE-GGA. The cyan circles are obtained with introduction of the *U* correction term. (b) Mapping between the two sets of couplings in the left panel.

although not trivial, as the two approximations are not equivalent (e.g., see ref 65). At each estimate V_{IF} of the coupling can be associated an error $cV_{IF}/(|a| + |b|)$,[23] which measures the maximal uncertainty (in fact, an upper bound for the uncertainty) due to departure from the two-state condition. Hence, a maximal error can be associated to the mean transfer integral by exploiting the well-known rules for independent error propagation. The estimates corresponding to the configurations after 33 000 and 51 000 simulation steps have been rejected because of a strong failure of the two-state model (i.e., $a^2 + b^2 < 0.75$, from which $c > 0.5$), resulting from localization of the transferring electron on different d-like MOs in the ET diabatic states and in the ground state of the system. Within the accuracy determined by the maximal error the PW91 and PBE exchange-correlation functionals yield the same mean value and root-mean-square (rms) value for the electronic coupling, that is $\langle V_{IF}\rangle_{PW91} = \langle V_{IF}\rangle_{PBE} = (23 \pm 3) \times 10^{-3}$ eV and $\sqrt{\langle V_{IF}^2\rangle_{PW91}} \equiv (V_{IF})_{rmsPW91} = (V_{IF})_{rmsPBE} = (37 \pm 7) \times 10^{-3}$ eV, respectively. The number of snapshots used to compute the averages is more than enough, as shown by the cumulative average in Figure 4b, according to which the mean value plateaus after six data points.

The difference between the two kinds of average is a consequence of the spreading of the results due to the dynamical nature of the water medium and clearly indicates that the inducing coordinate has been explored. In fact, water can affect the electronic coupling both by mediation of ET coupling pathways (mainly, through hydrogen bonds)[66,67] and by the electrostatic field determined around the two ions.[25] The magnitude of both effects can be strongly altered by the water displacements still allowed within the solvation cages, thus leading to the wide range of the transfer integral shown in Figure 4a. This range can be characterized by the standard deviation $\sigma_V = \sqrt{\langle V_{IF}^2\rangle - \langle V_{IF}\rangle^2} = 0.029$ eV, which is comparable with the mean values given above, as expected for flexible systems.[25,68] Indeed, the values of V_{IF} corresponding to different nuclear configurations can be viewed as "independent estimates" of the quantity $\langle V_{IF}\rangle$ (or $(V_{IF})_{rms}$). Thus, as an estimate of the mean value obtained after an infinite number of calculations, $\langle V_{IF}\rangle$ or $(V_{IF})_{rms}$ can be endowed with a statistical error $\sigma_{\langle V\rangle} = \sigma_V/\sqrt{18} = 0.007$ eV. Note that the two errors attributed to the mean transfer integral cannot be directly added.

As shown in the next section, the above value of the root-mean-square transfer integral is significantly larger than the experimental estimate derived from the ET Marcus' equation. This overestimation arises from the too fast asymptotic decay of the XC potential associated with the spurious self-interaction[69,70] because the d-like HOMO, essentially localized around one metal ion, has a too large tail on the other redox center. The correction of the charge distribution around the ions through the *U* term (and FON, whenever required) leads to the electronic couplings V_{IF}^U shown in Figure 5a. Relying on the matching between the results by PW91-GGA and PBE-GGA we employed only the PBE functional (used in the CPMD run of ref 30).

We note that for four of the selected MD configurations the DFT + *U* scheme yields the electronic coupling without the need for FON. However, as a consequence of the strong interdependence between energies and occupation numbers of the relevant orbitals in the employed Hubbard *U* correction (see eq 39 in Appendix B), for some MD configurations the plateau regime of the electronic coupling is reached only at very large values of σ, where a level scheme analogous to the one without the *U* correction term is recovered. In such cases, the maximal errors incidental to the smearing of the electronic charge, which are proportional to σ (see Appendix B, eqs 35 and 37), can be correspondingly large. In fact, the change in the density ensuing from the unduly large electron smearing can yield a significant orbital relaxation through the corresponding change in the KS effective potential (see eq 24). Thus, the transfer integrals corresponding to those plateaus are rejected, although the HOMO can be accidentally correct (as shown in Appendix B and the Supporting Information). Ultimately, we retain only the nine nuclear configurations whose transfer integrals are obtained either in the absence of FON or by plateaus that extend over σ ranges similar to the ones in Figure 1.

Although the amount of change in the transfer integral varies with the nuclear configuration, the sets of values V_{IF} and V_{IF}^U are correlated, as displayed by the mapping in Figure 5b. In fact, their correlation coefficient is $r_{V,V^U} = 0.81$, and the probability of finding an at least equal value of the coefficient if the two sets of data (each including nine points) are uncorrelated is $P_9(r \geq r_{V,V^U}) = 0.9\%$. This probability indicates a highly significant correlation[71] between the two sets of electron transfer integrals. Therefore, the relative values of the effective coupling obtained by means of eq 3 in the "bare" (without SIC) FON-DFT scheme are meaningful, on average, for the system under consideration. For example, the above conclusion supports the use of the bare

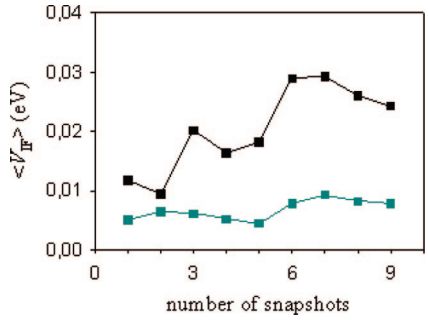

Figure 6. Dependence of the PBE-GGA mean transfer integral on the number of configurations used to compute the average. Cyan and dark squares are obtained by the FON-DFT approach with and without the *U* correction, respectively.

scheme in order to find the decay constant of the transfer integral with the distance between the two irons. Further analysis is required to ascertain the point. However, we wish to stress that eq 3, implemented within a bare DFT scheme, yielded a decay constant in good agreement with the empirical average packing density model[36] for the system studied in ref 23.

Using the *U* correction we obtain $\langle V_{IF}^U \rangle = 7.8 \times 10^{-3}$ eV and $(V_{IF}^U)_{rms} = 11.0 \times 10^{-3}$ eV. Both averages are endowed with the statistical error $\sigma_{\langle V \rangle}^U = 2.6 \times 10^{-3}$ eV. By comparison, the corresponding quantities obtained without the *U* correction by averaging on the reduced set of nuclear configurations are $\langle V_{IF} \rangle = 24 \times 10^{-3}$ eV, $(V_{IF})_{rms} = 34 \times 10^{-3}$ eV, and $\sigma_{\langle V \rangle} = 8 \times 10^{-3}$ eV. Their differences from the respective estimates based on 18 configurations are unimportant. The best estimate of the transfer integral and its standard error are considerably decreased using the *U* approach. However, we note that $(V_{IF}^U)_{rms}$ and $(V_{IF})_{rms}$ are of the same of order of magnitude, which is also attributable to the fact that eq 3 does not resort to any excited-state quantity, thus limiting the shortcomings of DFT.[23,69]

The significantly smaller standard deviation resulting from the *U*-corrected scheme is illustrated by the reduced spreading of the pertinent electronic coupling values (represented by cyan circles in Figure 5a) and results in a more rapid plateauing of the cumulative average transfer integral, as displayed by Figure 6. However, the statistical error continues to be relatively high. Actually, this is a common feature of high-level quantum chemical methods.[25,72] In fact, they generally reduce the systematic errors of the average quantities coming from the approximate description of the electronic structure, but hardly address the statistical errors since the number of data points used in the averaging is limited by their computational cost. Moreover, for a given number of points, the spreading of the results and thus the statistical error in the estimate of the mean transfer integral depend on the specific non-Condon effects characterizing the system under consideration. Ultimately, the higher accuracy of the FON-DFT + *U* computational scheme, relative to the FON-DFT scheme, pushes the spreading of the transfer integrals toward the correct one, exclusively determined by the failure of the Condon approximation.

The following points are worthy of note. (i) $(V_{IF}^U)_{rms}$ has a larger relative statistical error than $(V_{IF})_{rms}$, although its absolute statistical error is smaller. This is due to the physical limit in the spreading of the electronic couplings (expressing the departure from the Condon approximation) in conjunction with the overestimate of the root-mean-square (or mean) transfer integral without *U* correction. (ii) An exact (linear) correlation between the FON-DFT and FON-DFT + *U* results should imply the proportionality of the respective spreads. The achieved high correlation indicates a random contribution of the shortcomings in the electronic structure calculations employing the less accurate FON-DFT approach. The possible use of eq 3 in the bare DFT scheme, discussed above, essentially rests on such a random feature.

3.3. Coherence Parameter and Comparison with the Pathways Model. A quantity strictly related to σ_V is the coherence parameter $R_c = \langle V_{IF} \rangle^2 / \langle V_{IF}^2 \rangle$,[66] which gives a measure of the fluctuations in the transfer integral. The effect of the fluctuations is negligible when R_c is close to unity (so that the Condon approximation holds), while it is at a maximum when R_c approaches zero (breakdown of the Condon approximation). The latter case is typical of extremely flexible systems (although it can occur also in symmetry forbidden processes at the equilibrium nuclear configuration[34]). We obtain $R_c = 0.4$ (without the *U* correction) and $R_c^U = 0.5$. Both estimates reflect the fact that the solvation cages are far from the free-motion condition while still relatively far from a tight binding.

The value of the coherence parameter can be interpreted in terms of ET coupling pathways.[66,68] In fact, it is expected to be very small when the interaction between the donor and acceptor groups is mediated by several interfering coupling pathways, whereas it is close to unity in the case of a dominant-coupling pathway. The estimates of R_c for the system under consideration are relatively high, thus suggesting the presence of a dominant pathway. On the other hand, they are sufficiently far from unity so that a more complicated picture is necessary to describe some features of the ET system. To analyze the point we compare the ab initio electronic couplings V_{IF} and V_{IF}^U with the corresponding pathways products[73] T_{IF}, derived[74] using the pathway model.[16] In fact, according to this semiempirical model the electronic coupling is proportional to the product T_{IF} of the (coupling) decay factors for each step in the dominant pathway tube connecting the D and A groups. Each decay factor describes the exponential decay of the electronic coupling along a step. The pertaining decay constant depends on the through-bond, through-hydrogen-bond, or through-space character of the step. As the decay constant weighs the length of the corresponding step, a (unit-less) effective distance is associated to the dominant pathway and T_{IF} corresponds to the shortest effective distance between the redox centers.

In the solvated ferrous−ferric system with the face-to-face conformation the region between the ions comprises six waters (see Figure 2). Two of such water molecules (one from each ion complex) are always involved in the best pathway. The value of T_{IF} strongly increases when they are connected by a hydrogen bond (so that the through-space decay factor is replaced by the through-hydrogen-bond decay factor for one step along the best pathway). The mappings

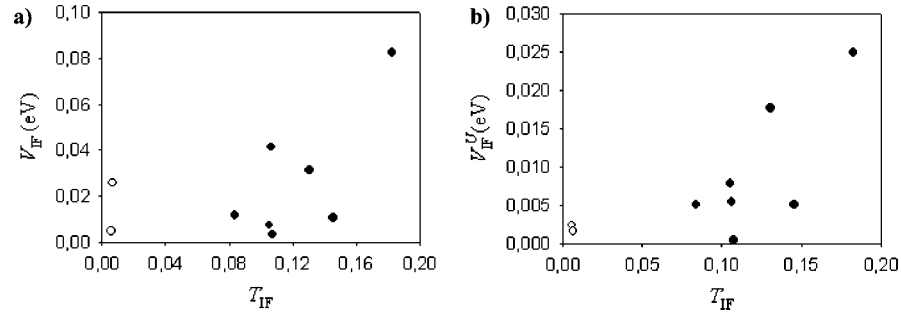

Figure 7. (a) FON-DFT electronic couplings (V_{IF}) and (b) FON-DFT + U electronic couplings (V_{IF}^{U}) vs pathway products (T_{IF}): (●) nuclear configurations including a hydrogen bond in the best ET pathway; (○) remaining configurations.

between the ab initio electronic couplings V_{IF} and V_{IF}^{U} and the products T_{IF} are shown in Figure 7a and 7b, respectively. The relative values of V_{IF} and T_{IF} have a similar spreading. In addition, the pathway couplings show a significant gap between the two nuclear configurations not including the hydrogen bond in the best ET pathway (empty circles) and the remaining ones (full circles). These two configurations yield a small coupling also in the ab initio U-corrected approach. The fact that other configurations, including the hydrogen bond in the best pathway, lead up to similarly small ab initio transfer integrals is attributable to the interplay between the bridging and electrostatic effects of the water environment, which is not grasped by the single-pathway picture.[25]

According to standard statistics[71] the correlation between the V_{IF} and T_{IF} sets is not significant, although appreciable, whereas the correlation between the U-corrected electronic couplings V_{IF}^{U} and the pathway products T_{IF} is significant.[75] In spite of the appreciable correlation between ab initio transfer integrals and pathway products, the dominant pathway can provide only an approximate picture of the electron-transfer pocess and cannot capture important features of the electronic structure. In fact, the scattering of the data points in Figure 7, the not-high level of correlation between the ab initio method and the semiempirical model, and the above argument about the ion−water electrostatic interactions (which can also comprise water molecules not directly involved in any tunneling pathway) point to the ab initio calculations with U correction as a reliable method for obtaining electronic couplings to be compared with experiment. Moreover, the ab initio method does not require the use of empirically adapted prefactors resting on the maximum ET rate constant as is the case when using the quantities T_{IF}.[76] Ultimately, let us stress that from the comparison between Figure 7a and 7b (where the solvent configurations characterized by an ET relevant hydrogen bond between the ions are in evidence) emerges the ability of the U correction to DFT in describing the effects of relevant hydrogen bonds on the transfer integral between the redox centers.

3.4. Comparison with Experiment. According to Marcus' ET theory the experimental estimate of the rms electronic coupling is obtained from eq 2 once the experimental value of the reorganization energy is inserted. The best estimates of ET rate constant and reorganization energy from the experimental data are[31,32] $k_{ET}^{(exp)} = 7.9 \times 10^2\ s^{-1}$ and $\lambda^{(exp)} = 2.1$ eV, respectively. The resulting transfer integral is $(V_{IF})_{rms}^{(exp)} = 7.1 \times 10^{-3}$ eV. The slightly larger value $(V_{IF}')_{rms}^{(exp)} = 7.3 \times 10^{-3}$ eV is obtained from the following refined expression for the rate constant[77]

$$k_{ET} = \nu_n \frac{1 - \exp(-\nu_{el}/2\nu_n)}{1 - \frac{1}{2}\exp(-\nu_{el}/2\nu_n)} \exp\left(-\frac{\lambda}{4k_B T}\right) \qquad (25)$$

where

$$\nu_{el} = \frac{\langle V_{IF}^2 \rangle}{\hbar} \sqrt{\frac{\pi}{\lambda k_B T}} \qquad (26)$$

is an electronic frequency for the electron transfer within the activated complex and ν_n is an effective nuclear frequency for the motion along the reaction coordinate. In eq 25 it is explicitly considered that the reaction free energy $\Delta G°$ is zero for an electron self-exchange reaction. Our ab initio best value for the rms transfer integral, provided with the statistical error (i.e., the uncertainty due to the finite number of data points used in the averaging), is $(V_{IF}^{U})_{rms} = (11.0 \pm 2.6) \times 10^{-3}$ eV. It can been seen that the discrepancy between the theoretical and the experimental best estimates is not statistically significant.[78] At any rate, the agreement can be considered good by taking into account the various steps connecting the observed rate constant of the bimolecular reaction and the electron self-exchange rate constant (e.g., the valuation of the pair distribution function). Moreover, the effective distance between the two ions is not necessarily a useful guide for assessing the magnitude of the transfer integral[15] due to the significant non-Condon effects here unraveled for the face-to-face conformation of the reactants.

As shown in Table 1, the ab initio estimate of the rms transfer integral obtained in the present work lies between the experimental value and two benchmark theoretical estimates in the literature.[3,5] The single-configuration value in ref 3, $V_{IF} = 98\ cm^{-1} = 12.2$ eV, refers to a reduced model system, which includes all ligands lying between the two metal ions, with a common value for the Fe−O distances in the ET complex. The estimate in eq 6 of ref 5, $V_{IF} = 124\ cm^{-1} = 15.3$ eV, rests on a simple model with one electron in the pseudopotential field of two ferric ions. The discrepancy between the latter and our theoretical estimate is beyond the assumed significance threshold, while we find a considerable agreement with the value in ref 3. On the other hand, the rms transfer integral obtained in the present work more closely approaches the experimental estimate. Moreover, it allows a statistical analysis of the remaining gap, also addressing the issue of the Condon approximation

Table 1. Comparison between Transfer Integral Best Estimates from Experimental Rates and from Different Theoretical Approaches

method	(model) system	V_{IF} (10^{-3} eV)	ref
	experimental, rms value		
from eq 2, $\lambda^{(exp)}$	$(Fe_{aq}-Fe_{aq})^{5+}$	7.1	31, 32
from eq 25, $\lambda^{(exp)}$	$(Fe_{aq}-Fe_{aq})^{5+}$	7.3	31, 32
	theoretical		
FON-DFT + U, rms value	$[Fe(H_2O)_6-Fe(H_2O)_6]^{5+}$	11.0 ± 2.6	present work
FON-DFT, rms value	$[Fe(H_2O)_6-Fe(H_2O)_6]^{5+}$	34 ± 8	present work
ROHF[a]	$[Fe(H_2O)_3-Fe(H_2O)_3]^{5+}$	12.2	3
fitting to Schrödinger equation solution	$Fe^{3+}-Fe^{3+}+e$	15.3	5

[a] Spin-restricted open-shell HF.

through the theoretical analysis on CPMD water configurations[79] (note that the CPMD simulations, performed at a suitably high ionic temperature, allowed reproducing the expected structure of the solvation shells and led to the right free-energy profile for the electron self-exchange process[30]).

By inserting the theoretical estimate of the reorganization energy in ref 31, $\lambda = 2.11$ eV, into eq 25 we can obtain a fully ab initio estimate of the self-exchange rate constant, that is $k_{ET}^{(theo)} = 15.5 \times 10^2\ s^{-1}$, with a confidence interval $(9.4-22.8) \times 10^2\ s^{-1}$, corresponding to the uncertainty interval for the electronic coupling. As a matter of fact, the electronic coupling affects the self-exchange rate approximately in a quadratic way (as is the case for eq 2) and the reorganization energy has a crucial role because of its presence in the (exponential) nuclear factor. As a consequence of these two circumstances, the absolute change in the ab initio rate constant, resulting from a difference in the employed set (λ, V_{IF}), is magnified relative to the latter (e.g., the best value of the rate constant resulting from the ab initio reorganization energy in ref 30, $\lambda' = 2.0$ eV, is $k_{ET}^{(theo)\prime} = 46.5 \times 10^2\ s^{-1}$). Therefore, the agreement between $k_{ET}^{(theo)}$ and $k_{ET}^{(exp)}$ can be considered quite good.

4. Conclusions

The main achievements of the present work are (i) a methodology to treat the thorny transition-metal redox system, (ii) theoretical analysis to justify a method that can be extended to other FON schemes, and (iii) an ab initio value of the root-mean-square transfer integral.

The use of a FON approach is crucial for computational treatment of the open-shell system under consideration. We provided the theoretical basis for the adopted computational methodology by suitable elaboration on the FON-DFT scheme with Gaussian broadening and subsequent exploitation of the formalism pertaining to the quantum theory of scattering by a potential. The resultant theoretical development transparently discloses the connections between the relevant quantities of the Kohn−Sham scheme with FON (namely, single-particle effective potential, energy eigenvalues, chemical potential, energy, entropy, and free energy associated to the fractional occupation numbers). Moreover, it describes the behavior of these quantities as a function of the Gaussian broadening over a wide range of the latter. In particular, a linear regime, characterizing the behavior of single-particle energies, chemical potential, and entropic contribution to the (variational) free energy, is identified and rationalized. The established connection between Gaussian broadening of the orbital occupations and orbital relaxation also provides a useful sufficient condition (corresponding to the linear regime of the KS levels) for future applications of the proposed FON method.

The linear regime of the KS single-particle energies is expected in the absence of orbital relaxation within the context of Janak's theorem.[55,80] In the present work it is formulated and extended to the behavior of other relevant KS quantities, within the context of the FON-DFT scheme with a Gaussian broadening, applied to open-shell transition-metal systems. Moreover, it is shown (Appendix B) that the relaxation of the orbitals is negligible beyond the linear response regime of the spin−orbital energies. It is worth noting that the provided theoretical analysis is amenable to extensions to different FON schemes with particular concern for the Fermi−Dirac broadening.[81]

Besides the FON approach, the ab initio U correction to DFT of ref 28 was essential for a reliable description of the electron charge distribution around the two redox centers, which in turn leads to correspondingly reliable estimates of the effective electronic couplings. Moreover, through the analysis of our results we can assert and quantify the limited adequacy of a single-tunneling pathway picture of the ET reaction. We also infer its limitations in describing the ET system under consideration because of the interplay between bridging and electrostatic effects of the water medium. Such limitations are, indeed, strictly related to the failure of the Condon approximation. In fact, the computed coherence parameter offers a common measure for both features. The analyzed departure from the Condon approximation supports two important points: (i) despite their lack of low-lying vacant orbitals, the water molecules can play a relevant role in ET to the extent that some ligand-to-metal charge transfer is present in the ground states of the reactants.[3] (ii) The nominal Fe-to-Fe distance (fixed in the present work) is not necessarily a useful guide for assessing (single) coupling magnitudes.[15]

The use of a recently proposed ab initio method for transfer integral valuation within the proposed FON-DFT approach along with the ab initio U correction[28,82] yields an estimate of the transfer integral for the solvated ferrous−ferric system that is in fair agreement with the experimental estimate derived from the observed kinetic data and reorganization energy.

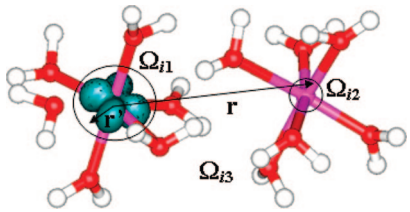

Figure 8. Partition of the space around the irons into three regions Ω_{ik} ($k = 1, 2, 3$). Ω_{i1} and Ω_{i2} denote suitable regions around the two metals where the ith MO is appreciable, and Ω_{i3} comprises all the space around. The HOMO of Figure 2a is represented. In the calculation of $I_{i1}(\mathbf{r};\sigma)$, $\mathbf{r}'$ spans Ω_{i1}.

Finally, we wish to stress that the present methodology offers a pragmatic approach for the quantitative investigation of electron self-exchange reactions in transition-metal systems.

Appendix A. Overview of the FON-DFT Scheme with Gaussian Broadening

The formal introduction of the fractional occupation numbers rests on the thermal DFT, founded by Mermin[83] through the extension of the Hohenberg−Kohn theorem to nonzero temperatures, within the grand canonical ensemble. In fact, at any finite temperature the Fermi−Dirac distribution leads to fractional occupations around the chemical potential μ (or the Fermi energy, ε_F, in the low-temperature limit, i.e., $k_BT \ll \varepsilon_F$). Then, the variational energy functional appropriate to FON-DFT is formally identical to the grand potential $\Omega = E - TS - \mu N$ of the finite-temperature DFT once an "entropy" is associated with the occupation numbers of the KS spin orbitals and is defined as[81]

$$S = -\sum_i [f_i \ln f_i + (1 - f_i)\ln(1 - f_i)] \tag{27}$$

although no physical meaning needs to be associated to the T (or k_BT) parameter. The same formalism is allowed by the other broadening functions[81,84,85] once the corresponding spreading parameter σ and occupation numbers are introduced, although σ has no simple physical interpretation.

If the total number of electrons N is fixed (i.e., in the canonical ensemble), the fictitious "free energy" $F = E - \sigma S$ is the suitable variational functional.[52] The stationary condition for Ω (or F) with respect to the occupation numbers f_i is written as

$$\frac{\partial \Omega}{\partial n_i} = \frac{\partial}{\partial n_i}(F - \mu N) = 0 \tag{28}$$

where the chemical potential is introduced as a Lagrange multiplier when using the free energy F. Note that by exploiting the property of the entropy[52] $\partial S/\partial f_i = (\varepsilon_i - \mu)/\sigma$ eq 28 yields Janak's theorem, that is $\partial E/\partial f_i = \varepsilon_i$.[80] Moreover, at zero temperature eq 28 leads to the classical FON solution,[38] according to which the levels with fractional occupation are degenerate and equal to ε_F.

In this work we use the Gaussian broadening scheme, so that the fractional occupations are given by

$$f_i(\sigma;\varepsilon_i - \mu) = 1 - \int_{-\infty}^{\varepsilon_i - \mu} g(\sigma;x)\,dx = \frac{1}{2}\mathrm{erfc}\left(\frac{\varepsilon_i - \mu}{\sigma}\right) \tag{29}$$

where erfc denotes the complementary error function. It is obtained from the Fermi occupation function at zero temperature by replacing the Dirac delta with its Gaussian broadening

$$g(\sigma;x) = \frac{1}{\sigma\sqrt{\pi}}\exp\left(-\frac{x^2}{\sigma^2}\right) \tag{30}$$

Appendix B. Fractional Occupations and Orbital Relaxation

In this appendix we elaborate on eq 24 in order to demonstrate that the ground-state wave function, used for evaluation of the transfer integral by means of eq 3, can be reliably obtained in a wide range of σ values, though the corresponding density is not physically meaningful.

First, it is worth noting that if v_{eff} undergoes an essentially homogeneous change as a consequence of the occupation broadening, the Hamiltonian operator correspondingly changes by an additive constant dependent only on σ. Therefore, the solutions $\bar{\varphi}_i(\mathbf{r};\sigma) = \varphi_i(\mathbf{r};0)$ are directly obtained from eq 20 and the KS eigenvalues $\varepsilon_i(\sigma)$ are uniformly shifted relative to $\varepsilon_i(0)$. In the general case the change in v_{eff} due to smearing of the electron charge depends on the space coordinate and is related to the kinetic energy and the chemical potential. To provide physical insight on this point let us consider a small variation $\delta n(\mathbf{r};\sigma)$ around the minimum density $n(\mathbf{r};\sigma)$, involving arbitrary changes in the shapes of the orbitals, while the occupation numbers are set at the values pertaining to the given equilibrium density. The corresponding functional derivative of the kinetic energy satisfies the equation[38,86]

$$\frac{\delta T[n(\sigma)]}{\delta n(\mathbf{r};\sigma)} = -v_{eff}(\mathbf{r};\sigma) + \mu(\sigma) \tag{31}$$

By writing eq 31 for zero smearing and subtracting term by term we get

$$\frac{\delta T[n(\sigma)]}{\delta n(\mathbf{r};\sigma)} - \frac{\delta T[n(0)]}{\delta n(\mathbf{r};0)} = -\Delta v_{eff}(\mathbf{r};\sigma) + \mu(\sigma) - \mu(0) \tag{32}$$

Equation 32 shows that the change in v_{eff} is independent of $\mathbf{r}$ if the functional derivative of the kinetic energy does or, at any rate, if $\delta T/\delta n$ is independent of σ. By considering the functional form of $T[n(\sigma)]$ it can be seen[56] that the term in the left-hand side of eq 32 is negligible compared to Δv_{eff} (which includes the change in the Coulomb potential) for small and delocalized density changes (involving also a variation of the total charge in ref 56). For the system under study, the changes in the electron density due to large enough values of σ (within the linear regime and beyond) are relatively dispersed around the two irons. Moreover, they do not entail a change in the total electronic charge and essentially involve d-like MOs (coming from atomic orbitals with the same quantum numbers), which are characterized by very similar orbital angular momenta, spatial extents, and thus kinetic energies (so that $T[n(\sigma)] \cong T[n(0)]$ at every σ). Consequently, the difference in the left-hand side of eq 32 is expected to be quite small over the entire σ range (especially at large enough σ). This working hypothesis (resting on the above physical arguments and corroborated by Figures 1 and 3) amounts to saying that although Δv_{eff}

generally depends on **r**, it continues to be of the order of magnitude of $\Delta\mu(\sigma) = \mu(\sigma) - \mu(0)$, that is a fraction of eV (e.g., at most 0.5 eV in the case of Figure 3b). The consequences of such a consideration on the integral of eq 24 can be well appreciated by partitioning the space around the redox centers as in Figure 8 and recasting eq 24 in the form

$$\bar{\varphi}_i(\mathbf{r};\sigma) = \varphi_i(\mathbf{r};0) + I_{i1}(\mathbf{r};\sigma) + I_{i2}(\mathbf{r};\sigma) + I_{i3}(\mathbf{r};\sigma) \quad (33)$$

with

$$I_{ik}(\mathbf{r};\sigma) = \frac{1}{2\pi\varphi_i(\mathbf{0};0)}\int_{\Omega_{ik}} \mathrm{d}^3r', \frac{\varphi_i(\mathbf{r}-\mathbf{r'};0)}{|\mathbf{r}-\mathbf{r'}|}[\Delta\varepsilon_i(\sigma) - \Delta v_{\mathrm{eff}}(\mathbf{r'};\sigma)]\bar{\varphi}_i(\mathbf{r'};\sigma) \quad (34)$$

Ω_{ik} ($k = 1, 2$) denote the regions where the ith MO is appreciably nonzero, while Ω_{i3} comprises all the space around. Such a partition rests on the consideration that with the ions 5.5 Å apart less than 1% of the relevant electron charge resides in the tunneling region between the two ions.[5] In accordance, a calculation based on the Schrödinger equation for the two ions without water molecules puts 98% of the electronic charge within 1.65 Å of one of the two ions.[5] In particular, as shown by Figure 8, the partition is meaningful for the HOMO, $\bar{\varphi}_{\mathrm{H}}(\mathbf{r};\sigma)$, which is the crucial molecular orbital in evaluating the transfer integral. In fact, both $\bar{\varphi}_{\mathrm{H}}(\mathbf{r};\sigma)$ and $\varphi_{\mathrm{H}}(\mathbf{r};0)$ are essentially localized on the same metal ion (named "ion 1" and depending on the sign of the energy difference ΔE_{IF} between the diabatic states) with a small tail on the other ion ("ion 2"). The accuracy in the determination of such a tail is the crucial factor in the calculation of the electronic coupling. However, even an excessive delocalization of the HOMO onto ion 2, responsible for a drastic overestimate of the transfer integral, corresponds to a negligible relative change of the orbital distribution around ion 1 once the localization of the orbital on the right ion (indicated by ΔE_{IF}) has been achieved. An analogous argument can be reported to the other orbitals. Consequently, it is a reliable approximation to replace $\bar{\phi}_i(\mathbf{r};\sigma)$ with $\phi_i(\mathbf{r};0)$ in the region Ω_{i1}, that is into the expression of $I_{i1}(\mathbf{r};\sigma)$, which amounts to applying the Born approximation[40,87] to eq 24. By focusing attention on the tail of the HOMO (so that **r** points toward the ferric ion 2 and $|\mathbf{r} - \mathbf{r}'|$ is on the order of the distance R between the two ions)[88] and dropping the explicit indication of the spin orbital in the quantities I_{ik} and Ω_{ik} we can write

$$I_1(\mathbf{r};\sigma) \lesssim \frac{1}{2\pi|\varphi_{\mathrm{H}}(\mathbf{0};0)|}\frac{|\varphi_{\mathrm{H}}(\mathbf{R};0)|}{R}|\Delta\varepsilon_{\mathrm{H}}(\sigma) - \Delta\mu(\sigma)|\frac{4}{3}\pi r_d^3 < |\varphi_{\mathrm{H}}(\mathbf{r'};0)|>_{\Omega_1} \approx A(N_d)\frac{2r_d^3}{3R}|\varphi_{\mathrm{H}}(\mathbf{r};0)|\sigma. \quad (35)$$

In eq 35 it is considered that $\langle|\varphi_{\mathrm{H}}(\mathbf{r'};0)|\rangle_{\Omega_1}$ is of the order of $|\varphi_{\mathrm{H}}(\mathbf{0};0)|$ and $\Omega_1 \approx 4/3\ \pi r_d^3$, where r_{d} is the Fe d-state radius. Moreover, the order of magnitude of $|\Delta\varepsilon_{\mathrm{H}} - \Delta\mu|$, i.e., $A(N_d)\sigma$, can be derived from eq 16 by considering that $\varepsilon_{\mathrm{H}} - \mu$ is an approximately linear function of σ and that $A(N_d)$ is much larger than $B\omega_{0j}$. As a matter of fact, the order of magnitude of $|\Delta\varepsilon_{\mathrm{H}} - \Delta\mu|$ remains the same within the σ range of nonlinear behavior described in the Supporting Information as well as when the quantities $B\omega_{0j}$ are appreciable, so that the differences among the slopes of the relative energies $\varepsilon_j - \mu$ cannot be disregarded. Therefore, eq 35 establishes a more general relation between the level shift and the orbital relaxation relative to the case of the uniform level shift. Using the value $r_d = 0.744$ Å, provided by the atomic-surface method,[89] and $N_d = 6$, the corrective factor for the HOMO ensuing from eq 35 is numerically equal to σ, as expressed in Ry. Therefore, the relative error due to neglecting $I_1(\mathbf{r};\sigma)$ in eq 33 is within a few percent, all the more that eq 35 actually supplies an upper bound for such an error. For example, since $R \gg \Omega_1^{1/3}$, by considering the case $\Delta v_{\mathrm{eff}}(\mathbf{r'};\sigma) \cong \Delta\mu(\sigma)\ \forall\mathbf{r'} \in \Omega_1$, we find

$$I_1(\mathbf{r};\sigma) \cong \frac{1}{2\pi\varphi_{\mathrm{H}}(\mathbf{0};0)}\frac{\varphi_{\mathrm{H}}(\mathbf{R};0)}{R}|\Delta\varepsilon_{\mathrm{H}}(\sigma) - \Delta\mu(\sigma)|\int_{\Omega_1}\bar{\varphi}_{\mathrm{H}}(\mathbf{r'};0)\mathrm{d}^3r' \cong 0 \quad (36)$$

since the positive and negative lobes of the d-like MO approximately cancel out in the integration. In general, the contribution of $I_1(\mathbf{r};\sigma)$ to the HOMO lies between the boundary provided by eqs 35 and 36 and can also be a nonmonotonic function of σ. The analog of eq 35 for the region Ω_2 is

$$I_2(\mathbf{r};\sigma) \lesssim A(N_d)\frac{r_t^2}{2\pi}|\varphi_{\mathrm{H}}(\mathbf{r};0)|\sigma \quad (37)$$

where r_t is some length, much smaller than r_d, measuring the size of Ω_2. Note that the approximations leading to eq 35 (in particular, the fact that Δv_{eff} and $\Delta\mu$ have the same order of magnitude) apply even better to the small region Ω_2, also considered that the Coulomb potential gives the major contribution to Δv_{eff}. By taking into account that $I_3(\mathbf{r};\sigma)$ is negligible by construction, from eqs 35, 36, and 37 we deduce that the HOMO and thus the transfer integral can be reliably evaluated at any σ since the onset of the linear regime. Note that the existence of a plateau of the transfer integral remains demonstrated by the fact that $\bar{\varphi}_{\mathrm{H}}(\mathbf{r};\sigma) \cong \varphi_{\mathrm{H}}(\mathbf{r};0) \cong \bar{\varphi}_{\mathrm{H}}(\mathbf{r};\sigma')$, for conveniently large σ and σ'. However, according to eqs 35, 36, and 37, the effects of the quantities $I_1(\mathbf{r};\sigma)$ and $I_2(\mathbf{r};\sigma)$ can become important for unduly large broadenings, where eq 16 also drastically fails. Then, $\bar{\varphi}_{\mathrm{H}}(\mathbf{r};\sigma)$ is no longer a good approximation to $\varphi_{\mathrm{H}}(\mathbf{r};0)$ and the ground-state wave function, ψ, is correspondingly wrong. Such a circumstance can be easily recognized by means of a considerable departure from the two-state condition $|\psi\rangle = a|\psi_{\mathrm{I}}\rangle + b|\psi_{\mathrm{F}}\rangle$, as measured by $c = \sqrt{1-a^2-b^2}$.

Appendix C. DFT + Hubbard *U* Approach to SIC

As mentioned in section 2.3, the approximate character of any currently available XC functional brings to the spurious electron self-interaction. In particular, the exchange potential does not have the correct inverse-distance asymptotic behavior; rather, it decreases exponentially with the distance

between the redox centers,[29] thus yielding a wrongly delocalized HOMO and a correspondingly overestimated electronic coupling. Self-interaction errors (whose importance can generally depend on the nature and configuration of the system under study) are not accounted for by eqs 35, 36, and 37, which delimit only the errors arising from electron smearing.

A substantial SIC rests on the appropriate treatment of the electronic correlation effects. Such effects can be expected to cancel, to a large extent, when the energy difference ΔE_{IF} between the diabatic states is computed. On the other hand, since the expected electronic coupling is much smaller than ΔE_{IF}, the delocalization of the transferring electron and thus the overlaps a and b of eq 3 can still be considerably affected.

In order to improve the description of the valence electron charge distribution (in particular, by taking properly into account the strong electron correlation effects) an orbital-dependent correction functional E_U, adapted from the Hubbard model[90] (dealing with strongly correlated electron systems), is added to the standard DFT functional E_{DFT}. According to the DFT + U approach, first introduced by Anisimov and co-workers,[91,92] a few localized orbitals (the d orbitals for the transition metals) are selected and the corresponding correlation is treated in a special way. The magnitude of E_U and thus the amount of the corrective electron correlation is controlled by the Hubbard U parameter, which measures the screened on-site Coulomb interaction. The total energy functional is written as

$$E_{DFT+U}[n] = E_U[\{n^{Is}_{mm'}\}] + E_{DFT}[n] \quad (38)$$

where I identifies the atomic site experiencing the Hubbard-like interaction (i.e., the ferric and ferrous species in the system under study), s denotes the electron spin,[93] m is the magnetic quantum number, and $\mathbf{n}^{Is}$ is the atomic orbital occupation matrix, which describes the degrees of freedom associated to the strongly correlated electrons on which the Hubbard U acts. In this work we adopt a rotationally invariant DFT + U scheme,[28,82] where the U parameter is obtained from first-principles, using a linear response approach internally consistent with the chosen definition for the occupation matrix.[28] The expression for E_U is

$$E_U[\{n^{Is}_{mm'}\}] = \frac{U}{2}\sum_{I,s} \mathrm{Tr}[\mathbf{n}^{Is}(1 - \mathbf{n}^{Is})] \quad (39)$$

which is described and detailed in ref 28. It is worth stressing that the Hubbard U computed within the scheme of ref 28 is not an empirical fitting parameter. It is a truly ab initio quantity, derived from the bare and screened linear responses of the system to a change in the occupation numbers.

The orbital-dependent correction potential changes the level structure because of the strict connection between level energy and occupation number embedded into eq 39. In the σ range corresponding to the linear regime the minority-spin (nominal) HOMO and LUMO are the only d-like MOs close in energy (0.01−0.3 eV) and with appreciable fractional occupation. They are lowered relative to the other levels corresponding to d-like MOs by an amount dependent on the nuclear configuration and the value of σ but generally of the order of 1−2 eV. This is is also the order of magnitude of the separation from the remaining lower lying and higher lying levels. Hence, the value $N_d = 2$ has to be used in the equations of section 2.4.

Acknowledgment. We thank Stefano Corni, Clotilde Cucinotta, Grace Brannigan, Giacomo Fiorin, Matteo Cococcioni, Nicola Marzari, and Paolo Giannozzi for helpful discussions. This work was supported by the NIH, grant no. GM 067689.

Supporting Information Available: Relaxation of the Condon approximation in the expression for the electron-transfer rate constant; derivation of the equations in section 2.5, further analytical development, and computational tests; transfer integral vs σ in the presence of the Hubbard U correction; table with the values of the electronic couplings and pathway products for the individual nuclear configurations. This material is available free of charge via the Internet at http://pubs.acs.org.

References

(1) Kuznetsov, A. M.; Ulstrup, J. *Electron Transfer in Chemistry and Biology*; John Wiley & Sons: New York, 1999.

(2) Brunschwig, B. S.; Logan, J.; Newton, M. D.; Sutin, N. *J. Am. Chem. Soc.* **1980**, *102*, 5798–5809.

(3) Logan, J.; Newton, M. D. *J. Chem. Phys.* **1983**, *78*, 4086–4091.

(4) Tembe, B. L.; Friedman, H. L.; Newton, M. D. *J. Chem. Phys.* **1982**, *76*, 1490–1507.

(5) Kuharski, R. A.; Bader, J. S.; Chandler, D.; Sprik, M.; Klein, M. L.; Impey, R. W. *J. Chem. Phys.* **1988**, *89*, 3248–3257.

(6) Rustad, J. R.; Rosso, K. M.; Felmy, A. R. *J. Chem. Phys.* **2004**, *120*, 7607–7615.

(7) Cui, D. Q.; Eriksen, T. E. *Environ. Sci. Technol.* **1996**, *30*, 2259–2262.

(8) Buerge, I. J.; Hug, S. J. *Environ. Sci. Technol.* **1998**, *32*, 2092–2099.

(9) Amonette, J. E.; Workman, D. J.; Kennedy, D. W.; Fruchter, J. S.; Gorby, Y. A. *Environ. Sci. Technol.* **2000**, *34*, 4606–4613.

(10) Nitzan, A. *Annu. Rev. Phys. Chem.* **2001**, *52*, 681–750.

(11) Marcus, R. A.; Sutin, N. *Biochim. Biophys. Acta* **1985**, *811*, 265–322.

(12) Newton, M. D. *Chem. Rev.* **1991**, *91*, 767–792.

(13) Landau, L. D. *Phys. Z. Sowjetunion* **1932**, *1*, 88–98. *ibid.* **1932**, 2, 46−51.

(14) Zener, C. *Proc. R. Soc. London A* **1932**, *137*, 696–702. *ibid.* 1933, 140, 660−668.

(15) Newton, M. D. *J. Phys. Chem.* **1988**, *92*, 3049–3056.

(16) Beratan, D. N.; Onuchic, J. N.; Hopfield, J. J. *J. Chem. Phys.* **1987**, *86*, 4488–4498.

(17) Farazdel, A.; Dupuis, M.; Clementi, E.; Aviram, A. *J. Am. Chem. Soc.* **1990**, *112*, 4206–4214.

(18) Cave, R. J.; Newton, M. D. *Chem. Phys. Lett.* **1996**, *249*, 15–19.

(19) Prezhdo, O. V.; Kindt, J. T.; Tully, J. C. *J. Chem. Phys.* **1999**, *111*, 7818–7827.

(20) Voityuk, A. A.; Rösch, N.; Bixon, M.; Jortner, J. *J. Phys. Chem. B* **2000**, *104*, 9740–9745.

(21) Stuchebrukhov, A. A. *Theor. Chem. Acc.* **2003**, *110*, 291–306.

(22) Prytkova, T. R.; Kurnikov, I. V.; Beratan, D. N. *J. Phys. Chem. B* **2005**, *109*, 1618–1625.

(23) Migliore, A.; Corni, S.; Di Flice, R.; Molinari, E. *J. Chem. Phys.* **2006**, *124*, 064501.

(24) Migliore, A.; Corni, S.; Di Felice, R.; Molinari, E. *J. Phys. Chem. B* **2006**, *110*, 23796–23800.

(25) Migliore, A.; Corni, S.; Di Felice, R.; Molinari, E. *J. Phys. Chem. B* **2007**, *111*, 3774–3781.

(26) Troisi, A.; Ratner, M. A.; Zimmt, M. B. *J. Am. Chem. Soc.* **2004**, *126*, 2215–2224.

(27) Bu, Y.; Wang, Y.; Xu, F.; Deng, C. *J. Mol. Struct. (Theochem)* **1998**, *453*, 43–48.

(28) Cococcioni, M.; de Gironcoli, S. *Phys. Rev. B* **2005**, *71*, 035105.

(29) Koch, W.; Holthausen, M. C. *A Chemist's Guide to Density Functional Theory*, 2nd ed.; Wiley-VCH Verlag GmbH: New York, 2000.

(30) Sit, P. H.-L.; Cococcioni, M.; Marzari, N. *Phys. Rev. Lett.* **2006**, *97*, 028303.

(31) Rosso, K. M.; Rustad, J. R. *J. Phys. Chem. A* **2000**, *104*, 6718–6725.

(32) Sutin, N. Theory of electron transfer reactions. In *Electron-transfer and electrochemical reactions. Photochemical reactions and other energized reactions*; Zuckermann, J. J., Ed.; VCH: New York, 1986; Vol. 15, p 16.

(33) Newton, M. D.; Sutin, N. *Annu. Rev. Phys. Chem.* **1984**, *35*, 437–480.

(34) Troisi, A.; Nitzan, A.; Ratner, M. A. *J. Chem. Phys.* **2003**, *119*, 5782–5788.

(35) Okuno, Y. *J. Chem. Phys.* **1999**, *111*, 8034–8038.

(36) Page, C. C.; Moser, C. C.; Chen, X.; Dutton, P. L. *Nature* **1999**, *402*, 47–52.

(37) Indeed, the poor convergence is a common feature for self-consistent field calculations on open-shell transition-metal systems both within the unrestricted or open-shell restricted Hartree−Fock (HF) and the unrestricted DFT approaches, see: Neese, F. *Chem. Phys. Lett.* **2000**, *325*, 93–98.

(38) Dreizler, R. M.; Gross, E. K. U. *Density functional theory*; Springer-Verlag: Berlin Heidelberg, 1990.

(39) For brevity, the spin dependence is not explicitly shown; however, the index i can be defined in such a way to distinguish the spin state.

(40) Cohen-Tannoudji, C.; Diu, B.; Laloë, F. *Quantum Mechanics*; Hermann: Paris, 1977; Vol. 2.

(41) Jamorski, C.; Martinez, A.; Castro, M.; Salahub, D. R. *Phys. Rev. B* **1997**, *55*, 10905–10921.

(42) Dunlap, B. I.; Rösch, N. *Adv. Quantum Chem.* **1990**, *21*, 317–339.

(43) Natiello, M. A.; Scuseria, G. E. *Int. J. Quantum Chem.* **1984**, *26*, 1039–1049.

(44) Springborg, M.; Albers, R. C.; Schmidt, K. *Phys. Rev. B* **1998**, *57*, 1427–1435.

(45) Görling, A. *Phys. Rev. A* **1996**, *54*, 3912–3915.

(46) Michelini, M. C.; Pis Diez, R.; Jubert, A. H. *Int. J. Quantum Chem.* **1998**, *70*, 693–701.

(47) Barcaro, G.; Fortunelli, A. *Faraday Discuss.* **2008**, DOI: 10.1039/b705105k. In the above article the HOMO−LUMO gap is derived from the nominal (fractionally occupied) HOMO and LUMO.

(48) Koopmans, T. *Physica* **1934**, *1*, 104–113.

(49) Luo, J.; Xue, Z. Q.; Liu, W. M.; Wu, J. L.; Yang, Z. Q. *J. Phys. Chem. A* **2006**, *110*, 12005–12009.

(50) Cardano, G. *Artis magnae, sive de regulis algebraicis*; Petrieus: Nuremberg, 1545.

(51) The validity of this consideration when σ approaches zero is clearly not affected by the fact that the HOMO can result from a wrong linear combination of d-like orbitals.

(52) Grotheer, O.; Fähnle, M. *Phys. Rev. B* **1998**, *58*, 13459–13464.

(53) According to the second-order energy correction in the stationary perturbation theory the mixing between two levels is determined not only by the difference between their unperturbed energies, but also by the matrix element of the perturbation Hamiltonian term between the corresponding orbital states. The latter depends also on the orbital localization. On the other hand, the KS level structure and the shapes of the orbitals reflect the approximate degeneracy of the two metal sites. Therefore, each level in the multiplet can mix in a similar way with couples of very close levels ε_k corresponding to symmetrically arranged orbitals.

(54) Kryachko, E. S.; Ludeña, E. V. *Energy density functional theory of many-electron systems*; Kluwer: Dordrecht, 1990.

(55) Beste, A.; Harrison, R. J.; Yanai, T. *J. Chem. Phys.* **2006**, *125*, 074101.

(56) Luo, J.; Yang, Z. Q.; Xue, Z. Q.; Liu, W. M.; Wu, J. L. *J. Chem. Phys.* **2006**, *125*, 094702.

(57) Slater, J. C. *The self-consistent field for molecules and solids*; McGraw-Hill: New York, 1974; Vol. 4.

(58) Car, R.; Parrinello, M. *Phys. Rev. Lett.* **1985**, *55*, 2471.

(59) Baroni, S.; Dal Corso, A.; de Gironcoli, S.; Giannozzi, P.; Cavazzoni, C.; Ballabio, G.; Scandolo, S.; Chiarotti, G.; Focher, P.; Pasquarello, A.; Laasonen, K.; Trave, A.; Car, R.; Marzari, N.; Kokalj, A. http://www.pwscf.org/.

(60) Perdew, J. P.; Chevary, J. A.; Vosko, S. H.; Jackson, K. A.; Pederson, M. R.; Singh, D. J.; Fiolhais, C. *Phys. Rev. B* **1992**, *46*, 6671–6687.

(61) Perdew, J. P.; Burke, K.; Ernzerhof, M. *Phys. Rev. Lett.* **1996**, *77*, 3865–3868.

(62) Knops-Gerrits, P. P.; Jacobs, P. A.; Fukuoka, A.; Ichikawa, M.; Faglioni, F.; Goddard, W. A., III *J. Mol. Catal. A: Chem.* **2001**, *166*, 3–13.

(63) (a) Ferretti, A.; Ruini, A.; Bussi, G.; Molinari, E.; Caldas, M. J. *Phys. Rev. B* **2004**, *69*, 205205. (b) Ferretti, A. DTI program, 2005; available from http://www.s3.infm.it/dti on request. Contact information: ferretti.andrea@unimore.it.

(64) Perdew, J. P.; Zunger, A. *Phys. Rev. B* **1981**, *23*, 5048–5079.

(65) Mattsson, A. E.; Armiento, R.; Schultz, P. A.; Mattsson, T. R. *Phys. Rev. B* **2006**, *73*, 195123.

(66) Balabin, I. A.; Onuchic, J. N. *Science* **2000**, *290*, 114–117.

(67) Lin, J.; Balabin, I. A.; Beratan, D. N. *Science* **2005**, *310*, 1311–1313.

(68) Prytkova, T. R.; Kurnikov, I. V.; Beratan, D. N. *Science* **2007**, *315*, 622–625.

(69) Ruiz, E.; Salahub, D. R.; Vela, A. *J. Phys. Chem.* **1996**, *100*, 12265–12276.

(70) Wu, Q.; Van Voorhis, T. *J. Chem. Phys.* **2006**, *125*, 164105.

(71) Taylor, J. R. *Introduzione all'analisi degli errori. Lo studio delle incertezze nelle misure fisiche*, 2nd ed.; Zanichelli: Bologna, 1999.

(72) Skourtis, S. S.; Balabin, I. A.; Kawatsu, T.; Beratan, D. N *Proc. Natl. Acad. Sci. U.S.A.* **2005**, *102*, 3552–3557.

(73) Jones, M. L.; Kurnikov, I. V.; Beratan, D. N. *J. Phys. Chem. A* **2002**, *106*, 2002–2006.

(74) The pathway products are computed by using Kurnikov's HARLEM program, which is available from http://www.kurnikov.org/.

(75) The correlation between ab initio transfer integrals and pathway products can be measured by the correlation coefficients, which are $r_{T,V} = 0.51$ and $r_{T,V^U} = 0.69$. The probabilities of finding at least equal values of those coefficients, if the corresponding data sets are uncorrelated, are $P_9(r \geq r_{T,V}) = 16\%$ and $P_9(r \geq r_{T,V^U}) = 4\%$, respectively. These values can be compared with the commonly accepted threshold of 5% for delimiting significant correlations. The two probabilities get closer to each other by excluding the two nuclear configurations not including the hydrogen bond in the best ET pathway. In fact, in this event we obtain $r_{T,V} = 0.73$ and $r_{T,V^U} = 0.76$, from which $P_7(r \geq r_{T,V}) = 6\%$ and $P_7(r \geq r_{T,V^U}) = 5\%$, respectively.

(76) Miyashita, O.; Okamura, M. Y.; Onuchic, J. N. *Proc. Natl. Acad. Sci. U.S.A.* **2005**, *102*, 3558–3563.

(77) Sutin, N. *Acc. Chem. Res.* **1982**, *15*, 275–282.

(78) The two estimates differ by about 1.4 standard deviations. The one-tail probability of obtaining a discrepancy which is at least 1.4 standard deviations is 8%. In other words, by assuming that our average value complies with a normal distribution centered on the expected (i.e., experimental) transfer integral, the probability that our single valuation of the rms electronic coupling gives a result at least as large as 11.0×10^{-3} eV is 8%. Therefore, according to the usual 5% criterion the discrepancy between the two values is not significant.

(79) In ref 3 the Condon approximation is tested on the apex-to-apex conformation by translating the reactants along the metal−metal direction.

(80) Janak, J. F. Proof that $\partial E/\partial n_i = \varepsilon_i$ in density-functional theory. *Phys. Rev. B* **1978**, *18*, 7165–7168.

(81) Weinert, M.; Davenport, J. W. *Phys. Rev. B* **1992**, *45*, 13709–13712.

(82) Cococcioni, M.; Dal Corso, A.; de Gironcoli, S. *Phys. Rev. B* **2003**, *67*, 094106.

(83) Mermin, N. D. *Phys. Rev.* **1965**, *137A*, 1441–1443.

(84) De Vita, A Ph.D. thesis, University of Keele, 1992.

(85) Elsässer, C.; Fähnle, M.; Chan, C. T.; Ho, K. M. *Phys. Rev. B* **1994**, *49*, 13975–13978.

(86) Takeda, R.; Yamanaka, S.; Yamaguchi, K. *Int. J. Quantum Chem.* **2003**, *93*, 317–323.

(87) Born, M. *Fisica Atomica*; Bollati Boringhieri: Torino, 1993.

(88) The argument can be suitably extended to the generic orbital. However, the analysis provided in the main text is appropriate for evaluation of the transfer integral.

(89) Harrison, W. A. *Elementary Electronic Structure*; World Scientific: Singapore, 1999.

(90) Hubbard, J. *Proc. R. Soc. A* **1963**, *276*, 238–257.

(91) Anisimov, V. I.; Zaanen, J.; Andersen, O. K. *Phys. Rev. B* **1991**, *44*, 943–954.

(92) Anisimov, V. I.; Solovyev, I. V.; Korotin, M. A.; Czyżyk, M. T.; Sawatzky, G. A. *Phys. Rev. B* **1993**, *48*, 16929–16934.

(93) The symbol *s* is here adopted, in place of the commonly used σ, to avoid confusion with the notation for the Gaussian broadening parameter.

CT800340V